Uselton

PITCH-, YAW-, AND ROLL-DAMPING CHARACTERISTICS
OF A SHUTTLE ORBITER AT $M_\infty = 8$

Bob L. Uselton and Leroy M. Jenke
ARO, Inc.

VON KÁRMÁN GAS DYNAMICS FACILITY
ARNOLD ENGINEERING DEVELOPMENT CENTER
AIR FORCE SYSTEMS COMMAND
ARNOLD AIR FORCE STATION, TENNESSEE 37389

May 1975

Final Report for Period June 24 — July 26, 1974

Prepared for

NASA-LANGLEY RESEARCH CENTER
HAMPTON, VIRGINIA 23365

NOTICES

When U. S. Government drawings specifications, or other data are used for any purpose other than a definitely related Government procurement operation, the Government thereby incurs no responsibility nor any obligation whatsoever, and the fact that the Government may have formulated, furnished, or in any way supplied the said drawings, specifications, or other data, is not to be regarded by implication or otherwise, or in any manner licensing the holder or any other person or corporation, or conveying any rights or permission to manufacture, use, or sell any patented invention that may in any way be related thereto.

Qualified users may obtain copies of this report from the Defense Documentation Center.

References to named commercial products in this report are not to be considered in any sense as an endorsement of the product by the United States Air Force or the Government.

This report has been reviewed by the Information Office (OI) and is releasable to the National Technical Information Service (NTIS). At NTIS, it will be available to the general public, including foreign nations.
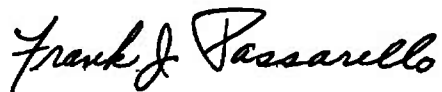
APPROVAL STATEMENT

This technical report has been reviewed and is approved for publication.

FOR THE COMMANDER

JIMMY W. MULLINS
Lt Colonel, USAF
Chief Air Force Test Director, VKF
Directorate of Test

FRANK J. PASSARELLO
Colonel, USAF
Director of Test

UNCLASSIFIED

REPORT DOCUMENTATION PAGE		READ INSTRUCTIONS BEFORE COMPLETING FORM
1 REPORT NUMBER AEDC-TR-74-129	2. GOVT ACCESSION NO.	3 RECIPIENT'S CATALOG NUMBER
4 TITLE (and Subtitle) PITCH-, YAW-, AND ROLL-DAMPING CHARACTER- ISTICS OF A SHUTTLE ORBITER AT $M_\infty = 8$		5 TYPE OF REPORT & PERIOD COVERED Final Report–June 24 – July 26, 1974
		6 PERFORMING ORG. REPORT NUMBER
7 AUTHOR(s) Bob L. Uselton and Leroy M. Jenke, ARO, Inc.		8. CONTRACT OR GRANT NUMBER(s)
9 PERFORMING ORGANIZATION NAME AND ADDRESS Arnold Engineering Development Center (XO) Arnold Air Force Station, Tennessee 37389		10. PROGRAM ELEMENT, PROJECT, TASK AREA & WORK UNIT NUMBERS Program Element 921E Project 9692
11 CONTROLLING OFFICE NAME AND ADDRESS NASA-Langley Research Center Hampton, Virginia 23365		12. REPORT DATE May 1975
		13. NUMBER OF PAGES 33
14 MONITORING AGENCY NAME & ADDRESS(if different from Controlling Office)		15. SECURITY CLASS. (of this report) UNCLASSIFIED
		15a. DECLASSIFICATION/DOWNGRADING SCHEDULE N/A

16 DISTRIBUTION STATEMENT (of this Report)

Approved for public release; distribution unlimited.

17 DISTRIBUTION STATEMENT (of the abstract entered in Block 20, if different from Report)

18 SUPPLEMENTARY NOTES

Available in DDC

19 KEY WORDS (Continue on reverse side if necessary and identify by block number)

damping	characteristics
pitch (motion)	089B Shuttle Orbiter
yaw	Mach number
roll	Reynolds numbers

20 ABSTRACT (Continue on reverse side if necessary and identify by block number)

Wind tunnel tests were conducted for NASA-Langley at $M_\infty = 8$ to determine the pitch-, yaw-, and roll-damping characteristics of a modified 089B shuttle orbiter configuration. Data were obtained utilizing the small-amplitude forced-oscillation technique at angles of attack of -4.9 to 26.5 deg at Reynolds numbers, based on model length, of 1.18×10^6 to 4.82×10^6. The orbiter was dynamically stable in pitch, yaw, roll, and statically unstable

DD $_{1\ JAN\ 73}^{FORM}$ 1473　EDITION OF 1 NOV 65 IS OBSOLETE

UNCLASSIFIED

20. ABSTRACT (Continued)

in yaw for the moment reference of the test configurations. The pitch derivatives were dependent on Reynolds number while the roll derivatives were independent of Reynolds number.

AFSC
Arnold AFS Tenn

PREFACE

The work reported herein was conducted by the Arnold Engineering Development Center (AEDC), Air Force Systems Command (AFSC), for NASA-Langley Research Center under Program Element 921E, Project 9692. NASA-Langley project monitor was Mr. Delma C. Freeman, Jr. The results presented herein were obtained by ARO, Inc. (a subsidiary of Sverdrup & Parcel and Associates, Inc.), contract operator of AEDC, AFSC, Arnold Air Force Station, Tennessee. The tests were conducted on June 24, 1974 and July 26, 1974 under ARO Project Nos. VA498 and V41B-48A. The final data package was completed on August 26, 1974, and the manuscript (ARO Control No. VKF-TR-74-100) was submitted for publication on October 16, 1974.

CONTENTS

ILLUSTRATIONS

Figure

TABLES

1.0 INTRODUCTION

Previous test programs have been conducted by NASA-Langley to measure the dynamic derivatives of the shuttle orbiter. The majority of these programs have been conducted in Langley facilities at Mach numbers from 0.3 through 4.6 (Refs. 1 and 2). In order to extend the range of measured derivatives into the hypersonic speed regime, NASA-Langley sponsored a test program at the von Kármán Gas Dynamics Facility (VKF). The purpose of the test program was to measure the pitch-, yaw-, and roll-damping derivatives of a shuttle orbiter configuration at Mach number 8. The test configuration was a 0.012-scale model of a modified 089B orbiter. Data were obtained at Reynolds numbers (based on model length) of 1.18×10^6 through 4.82×10^6. The angle of attack was varied from -4.9 to 26.5 deg, and values of the reduced frequency parameter varied from 0.0033 to 0.011. The small-amplitude forced-oscillation technique was utilized.

2.0 APPARATUS

2.1 MODEL

The orbiter model (Fig. 1) was designed and fabricated by NASA-Langley. The stainless steel model was a 0.012-scale model of a modified 089B orbiter configuration. The modification to the model consisted of using a 139B nose on the 089B body (see Fig. 2). Tests were conducted with body flap off, the rudder flare angle = 40 deg, and the elevons set at zero (Configuration 1). The orbiter was also tested without the vertical tail (Configuration 2). The configurations were balanced about the flexure pivot axis for the pitch tests and about the roll axis for the roll tests. Model details are shown in Fig. 2.

2.2 TEST MECHANISM

2.2.1 Pitch-/Yaw-Damping Mechanism

The VKF 1.B pitch-/yaw-damping test mechanism (Fig. 3) (Ref. 3) utilizes a cross-flexure pivot, an electric shaker motor, and a one-component moment beam which is instrumented with strain gages to measure the forcing moment of the shaker motor.

The motor is coupled to the moment beam by means of a connecting rod and flexural linkage which converts the translational force to a moment (70 in.-lb maximum) to oscillate the model at amplitudes up to ±3 deg (depending on flexure balance) and frequencies from 2 to 20 Hz. The cross flexures, which are instrumented to measure the pitch/yaw displacement, support the model loads and provide the restoring moment to cancel the inertia moment when the system is operating at its natural frequency. Presently, two cross-flexure balances exist and each is composed of three beams with single unit construction. The beam thicknesses for the balances are 0.087 and 0.171 in., and the restoring moments produced by the balances are -132 and -938 ft-lb/radian, respectively. Since the moment beam which is used to measure the forcing moment is not subjected to the static loads, it can be made as sensitive as required for the dynamic measurements. Beams exist which can measure up to ±0.6, ±3, ±11, ±25. and ±70 in.-lb. A pneumatic- and spring-operated locking device is provided to hold the model during injection into or retraction from the tunnel or during tunnel starts. The cross-flexure balances can be supported by an elliptical cross-section sting (provides support strength and maximum model clearance but is not water-cooled) or a 1.75-in.-diam water-cooled sting (normally used with the roll-damping balance). The water-cooled sting was used during the present tests in conjunction with the -132 ft-lb/radian cross-flexure balance and primarily the ±3 in.-lb moment beam.

2.2.2 Roll-Damping Mechanism

The VKF 1.D roll-damping test mechanism (Fig. 4) (Ref. 4) utilizes a water-jacketed, five-component balance, twin beam flexures, roller bearings to support the loads, and two electric printed-circuit drive motors. The motors are directly coupled to the balance and supply up to 120 in.-lb roll moment to oscillate the system at amplitudes up to ±3 deg and frequencies from 2 to 20 Hz. The twin beam flexures mount from the stationary sting to the oscillating water jacket and provide a restoring moment which cancels the intertia moment when the system is operating at the natural frequency of the model-flexure system. The flexures are instrumented to measure the roll displacement. The entire mechanism is water-cooled to permit testing in the hypersonic tunnels.

Two five-component balances have been fabricated for the system to provide good balance sensitivity over the load range. Both balances utilize outrigger beams in the yaw sections and thin-ribbed flexures in

the roll section to provide sensitive yaw and roll outputs while maintaining large normal-force capacity and rigidity in yaw. Semiconductor gages are also utilized for the yaw and roll sections for additional sensitivity. The -59 balance was used during the present test and the load capacity of both balances is listed as follows:

Balance	Normal Force, lb	Pitching Moment, in.-lb	Side Force, lb	Yawing Moment, in.-lb	Rolling Moment, in.-lb
-59	500	1125	40	84	10
-60	1200	2700	100	210	100

2.3 INSTRUMENTATION

The forced-ocillation instrumentation (Refs. 3 and 4) utilizes an electronic analog system with precision electronics. The control, monitor, and data acquisition instrumentation is contained in a portable console that can be easily interfaced with the instrumentation of the various tunnels.

The control instrumentation provides a system which can vary the oscillation frequency, oscillation amplitude, and angular position (θ, ψ or ϕ) of the model within the flexure limits. The oscillation amplitude is controlled by an electronic feedback loop which permits testing of both dynamically stable and unstable configurations.

Data are normally obtained at or near the natural frequency of the model flexure system; however, the electronic resolvers used permit data to be obtained off resonance. All gages are excited by d-c voltages and outputs are increased to optimum values by d-c amplifiers. Typical balance outputs from an oscillating model are composed of oscillatory components (OC) superimposed on static components (SC). These components are separated in the data system by bandpass and lowpass filters. The SC outputs are sent directly to the tunnel scanner and computer, which for the pitch/yaw tests calculate the static pitching-moment coefficient C_m (C_n) and sting deflections and for the roll test calculate the static force and moment coefficients, C_N, C_m, C_Y, C_n and C_ℓ. The OC outputs are input to the resolver instrumentation and precise frequency measuring instrumentation. The resolvers utilize very accurate analog electronic devices to process the OC signals and output d-c voltages. During the pitch/yaw tests the output d-c voltages are proportional to the amplitude squared, the in-phase

and quadrature (90 deg out of phase) balance components (forcing torque) and the in-phase and quadrature sting components. For the roll-damping tests, the output d-c voltages are proportional to the amplitude squared, the in-phase and quadrature rolling moments, and the quadrature yawing moments. A switch is also provided in the resolver system to bypass the phase shift network so that the in-phase yawing moments can be determined. The resolver and frequency outputs are read by the tunnel scanner and sent to the computer. The frequency instrument controls the length of the data interval in increments from approximately 2 to 60 seconds, during which time the scanner reads each input approximately 10 times per second. The average values of the readings are calculated by the computer, which then uses these average values to calculate the dynamic coefficients (1) pitch/yaw tests, $C_{m_q} + C_{m_{\dot\alpha}}$ ($C_{n_r} - C_{n_{\dot\beta}} \cos \alpha$) and C_{m_α} ($C_{n_\beta}\cos \alpha$) (2) roll tests, $C_{\ell_p} + C_{\ell_{\dot\beta}} \sin \alpha$, $C_{n_p} + C_{n_{\dot\beta}} \sin \alpha$ and $C_{Y_p} + C_{Y_{\dot\beta}} \sin \alpha$. The method used to reduce the data may be found in Refs. 3, 4, and 5.

2.4 WIND TUNNEL

Hypersonic Wind Tunnel (B) is a continuous, closed-circuit, variable density wind tunnel with two axisymmetric contoured nozzles and a 50-in.-diam test section. The tunnel can be operated at a nominal Mach number of 6 or 8 at stagnation pressures from 20 to 300 and 50 to 900 psia, respectively, at stagnation temperatures up to 1350°R. The model may be injected into the tunnel for a test run and then retracted for model cooling or model changes without stopping the tunnel flow. Tunnel details are shown in Fig. 5.

3.0 PROCEDURE AND PRECISION OF DATA

3.1 TEST CONDITIONS

The nominal wind tunnel test parameters at which the data were obtained are presented in Table 1, and summaries of test configurations for the pitch, yaw, and roll tests are presented in Table 2.

3.2 TEST PROCEDURE

The model was oscillated at a constant oscillation amplitude of ±1 deg for the pitch- and yaw-damping tests and ±2 deg during the roll-damping tests.

3.3 PRECISION OF DATA

Uncertainties (bands which include 95 percent of the calibration data) in the basic tunnel parameters (p_O, T_O, and M_∞) were estimated from repeat calibrations of the instrumentation and from repeatability and uniformity of the test section flow during tunnel calibrations. These uncertainties were used to estimate uncertainties in other free-stream properties using a Taylor series method of error propagation (Ref. 6). The estimated uncertainties are as follows:

Tunnel Parameters Uncertainty

$Re_\ell \times 10^{-6}$	$\Delta(M_\infty)$	$\Delta(Re_\ell \times 10^{-6})$	$\Delta(q_\infty)$ psia	$\Delta(V_\infty)$ ft/sec
1.18	±0.024	±0.011	±0.013	±9.5
2.35		±0.022	±0.026	
3.52		±0.033	±0.040	
4.82		±0.045	±0.056	

The balances for the pitch-, yaw-, and roll-damping tests were calibrated before and after the tests, and check calibrations were made during the test. Sting bending effects utilizing the technique illustrated in Ref. 7 were used in the data reduction of the pitch-and yaw-damping derivatives. Uncertainties in the measurements of sting effects were included in the error analysis. Structural damping values were obtained at vacuum conditions before the tunnel entry to evaluate the still-air damping contribution. The uncertainties in the balance and data system were combined with uncertainties in the tunnel parameters assuming a Taylor series method of error propagation (Ref. 6) to estimate the precision of the aerodynamic damping coefficients. The estimated uncertainties are as follows:

Pitch-Damping Uncertainty

Config.	$Re_\ell \times 10^{-6}$	α, deg	$C_{m_q} + C_{m_{\dot\alpha}}$	$\Delta(C_{m_q} + C_{m_{\dot\alpha}})$	C_{m_α}	$\Delta(C_{m_\alpha})$
1	1.18	-0.4	-1.0	±0.13	0.05	±0.026
	1.18	7.4	-1.3	±0.13	0.13	±0.026
	2.35	1.0	-0.7	±0.07	0.05	±0.013
	2.35	25.0	-2.5	±0.09	-0.06	±0.013
	4.82	2.3	-0.8	±0.04	0.05	±0.006
	4.82	23.9	-2.4	±0.06	-0.10	±0.008

Yaw-Damping Uncertainty

Config.	$Re_\ell \times 10^{-6}$	α, deg	$C_{n_r} - C_{n_{\dot\beta}} \cos \alpha$	$\Delta(C_{n_r} - C_{n_{\dot\beta}} \cos \alpha)$	$C_{n_\beta} \cos \alpha$	$\Delta(C_{n_\beta} \cos \alpha)$
1	2.35	0	-0.78	±0.026	-0.04	±0.007
1		25.3	-0.23	±0.019	-0.10	±0.007
2	↓	0	-0.30	±0.018	-0.09	±0.007
2		25.3	-0.22	±0.018	-0.11	±0.007

Roll-Damping Uncertainty

Config.	$Re_\ell \times 10^{-6}$	α, deg	$C_{\ell_p} + C_{\ell_{\dot\beta}} \sin \alpha$	$\Delta(C_{\ell_p} + C_{\ell_{\dot\beta}} \sin \alpha)$
1	1.18	0	-0.11	±0.027
	1.18	24	-0.21	±0.028
	2.35	0	-0.11	±0.014
	2.35	24	-0.27	±0.016
	3.52	0	-0.12	±0.010
	3.52	26	-0.24	±0.011
	4.82	0	-0.12	±0.008
	4.82	26	-0.24	±0.009
2	2.35	0	-0.09	±0.013
	2.35	26	-0.28	±0.015
	4.82	0	-0.10	±0.007
	4.82	26	-0.22	±0.006

Static Data Uncertainty

Config.	$Re_\ell \times 10^{-6}$	$\Delta(C_{N_1})$	$\Delta(C_{N_2})$	$\Delta(C_{m_1})$	$\Delta(C_{m_2})$
1 and 2	1.18	±0.019	±0.022	±0.010	±0.010
	2.35	±0.010	±0.014	±0.005	±0.005
	3.52	±0.006	±0.012	±0.004	±0.004
	4.82	±0.005	±0.011	±0.002	±0.003

[1]Near minimum values.
[2]Near maximum values.

Uncertainties for $C_{n_p} + C_{n_{\dot{\beta}}} \sin \alpha$ were not quoted since the accuracy of these measurements in the wind tunnel (where tunnel facility vibrations and unsteady flow fluctuations are a problem) are unknown. However, in the ideal laboratory environment, it has been shown in Ref. 4 that this parameter can be measured accurately. Before the confidence level of the wind tunnel measurement of $C_{n_p} + C_{n_{\dot{\beta}}} \sin \alpha$ can be determined, a simple aerodynamic shape designed to certain specifications (zero products of inertia) especially for these type tests will have to be tested. The orbiter model was not designed to obtain the $C_{n_p} + C_{n_{\dot{\beta}}} \sin \alpha$ data which was a secondary measurement.

Measurements of the model pitch are precise within ±0.05 deg, based on repeat calibrations. Model attitude corrections were made for model-balance deflections under air load, and the precision of the calculated model angle is estimated to be ±0.1 deg.

4.0 RESULTS AND DISCUSSION

Figure 6 shows the normal-force and pitching-moment coefficients as a function of angle of attack for configuration 1 (orbiter) and configuration 2 (without vertical tail) at several Reynolds numbers. The normal-force coefficient showed no measurable effect of Reynolds number. The pitching-moment coefficients did show some measurable effect of Reynolds number at $\alpha > 8$ deg. The static data also showed that neither configuration trimmed at the angles of attack tested for the reference center of gravity of this particular configuration.

The pitch-stability derivatives as a function of angle of attack for configuration 1 are shown in Fig. 7 at Reynolds numbers, based on model length, of 1.18×10^6, 2.35×10^6, and 4.81×10^6. The orbiter was dynamically stable in pitch, and the damping derivatives generally increased with angle of attack. For $Re_\ell = 2.35 \times 10^6$ and 4.81×10^6 the slope of the pitching-moment curve showed variation with angle of attack and changed from a positive to negative slope in the 12- to 18-deg angle-of-attack range. The significant Reynolds number effect occured in the -2 to 2 deg angle-of-attack range where the pitch damping decreased with increasing Reynolds number. The slope of the pitching-moment curve generally became more stabilizing with increasing Reynolds number.

Figure 8 shows the yaw-stability derivatives as a function of angle of attack for configurations 1 and 2 at $Re_\ell = 2.34 \times 10^6$. Both configurations were dynamically stable and the damping derivatives were generally invariant for angles of attack above 5 deg. An increase in model damping occurred at the lower angles of attack, particularly for the orbiter configuration. The yawing-moment coefficient due to sideslip angle ($C_{n_\beta} \cos \alpha$) shows both configurations to be statically unstable in yaw for the moment reference of this particular configuration. Increasing angle of attack increased the static instability of the orbiter and didn't affect the instability of the orbiter without the vertical tail (configuration 2). Removal of the vertical tail decreased model damping at the lower angles of attack $-3 \leq \alpha \leq 3$ deg as expected and didn't produce any large effects for angles of attack greater than 3 deg. For angles of attack up to 20 deg, the static instability increased with the removal of the vertical tail.

The roll-damping derivatives are presented in Fig. 9 for configurations 1 and 2 at several Reynolds numbers. The derivatives generally increased with angle of attack. Varying Reynolds number didn't produce any large effects on the roll-damping derivatives. The roll-damping increment due to vertical tail is shown in Fig. 10 for Reynolds numbers 2.3×10^6 and 4.7×10^6. As expected, removing the vertical tail generally decreased model damping slightly.

The pitch-, yaw-, and roll-damping derivatives for configurations 1 and 2 are presented as a function of Mach number for $\alpha = 0$ in Fig. 11. The supersonic data (Ref. 2) were obtained by NASA-Langley in the Langley Unitary Plan Wind Tunnel on a 0.0165-scale model. The damping derivatives decreased with increasing Mach number with the exception of the yaw derivatives for configuration 1. The data indicate a significant increase in the yaw damping from the Langley data at $M_\infty \approx 5$ to the AEDC data at $M_\infty = 8$ for configuration 1; however, the tail-off data (configuration 2) does not indicate any substantial difference. Thus, the main difference is that the AEDC data show that the vertical tail adds to the yaw damping at $\alpha = 0$ where the tail is not blocked out by the body wake, while the NASA data show essentially no effect of vertical tail on yaw damping. There is a Re_ℓ difference between the two sets of data which may be a contributing factor as was seen in the pitch data (see Fig. 7). Otherwise, no reason for this difference is known.

Figure 12 presents the yawing-moment derivatives due to roll rate as a function of angle of attack for both configurations at several Reynolds numbers. The derivatives varied considerably with angle of

attack. Additional discussion isn't warranted since the validity of this technique has not been fully verified (see Section 3.3).

5.0 CONCLUSIONS

Wind tunnel tests were conducted to determine the pitch-, yaw-, and roll-damping characteristics of the modified 089B shuttle orbiter configuration. Also, the effect of the vertical tail on the yaw and roll derivatives was investigated. Data were obtained at Mach number 8 at free-stream Reynolds numbers, based on model length, of 1.18 x 10^6 to 4.82 x 10^6. Conclusions based on the results presented in this report are given below.

1. The orbiter is dynamically stable in pitch, yaw, and roll, and statically unstable in yaw.

2. In general, the pitch- and roll-damping derivatives increase with angle of attack while the yaw-damping derivatives are essentially invariant with angle of attack for $\alpha > 5$ deg.

3. The pitch derivatives of the orbiter are strongly dependent on Reynolds number at the lower angles of attack ($-3 \leq \alpha \leq 3$ deg) while variation of Reynolds number produces no large effects on the roll-damping derivatives, normal-force coefficients, or pitching-moment coefficients.

4. Removing the vertical tail: (1) decreases the yaw-damping derivatives at the lower angles of attack ($-3 \leq \alpha \leq 3$ deg), (2) decreases slightly the roll-damping derivatives at the majority of the angles of attack tested, and (3) increases the static instability in yaw.
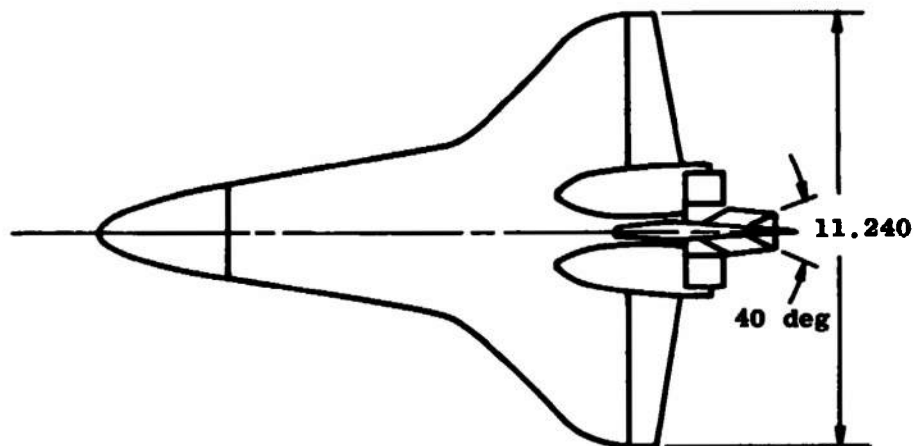
REFERENCES

1. Boyden, R. P. and Freeman, Delma C. "Subsonic and Transonic Dynamic Stability of a Modified 089B Shuttle Orbiter." NASA-TMX-72631, January 1975.

2. Freeman, Delma C., Boyden, Richmond P., and Davenport, E. E. "Supersonic Dynamic Stability of a Modified 089B Shuttle Orbiter." NASA-TMX-72630, October 1974.

13

3. Burt, G. E. "A Description of a Pitch/Yaw Dynamic Stability, Forced-Oscillation Test Mechanism for Testing Lifting Configurations." AEDC-TR-73-60 (AD762286), June 1973.

4. Burt, G. E. "A Description of a Forced-Oscillation Test Mechanism for Measuring Dynamic-Stability Derivatives in Roll." AEDC-TR-73-49 (AD762258), June 1973.

5. Schueler, C. J., Ward, L. K., and Hodapp, A. E., Jr. "Techniques for Measurements of Dynamic-Stability Derivatives in Ground Test Facilities." AGARDograph 121 (AD669227), October 1967.

6. Beers, Yardley. Introduction to the Theory of Error. Addison-Wesley Publishing Company, Inc., Reading, Mass., 1957, pp. 26-36.

7. Burt, G. E. and Uselton, James C. "Effect of Sting Oscillations on the Measurement of Dynamic Stability Derivatives in Pitch and Yaw." AIAA Paper 74-612, Presented at the AIAA 8th Aerodynamics Testing Conference, Bethesda, Maryland, July 1974.
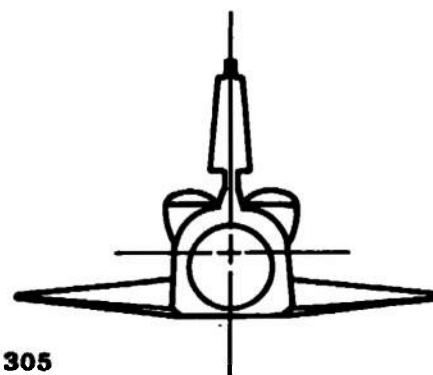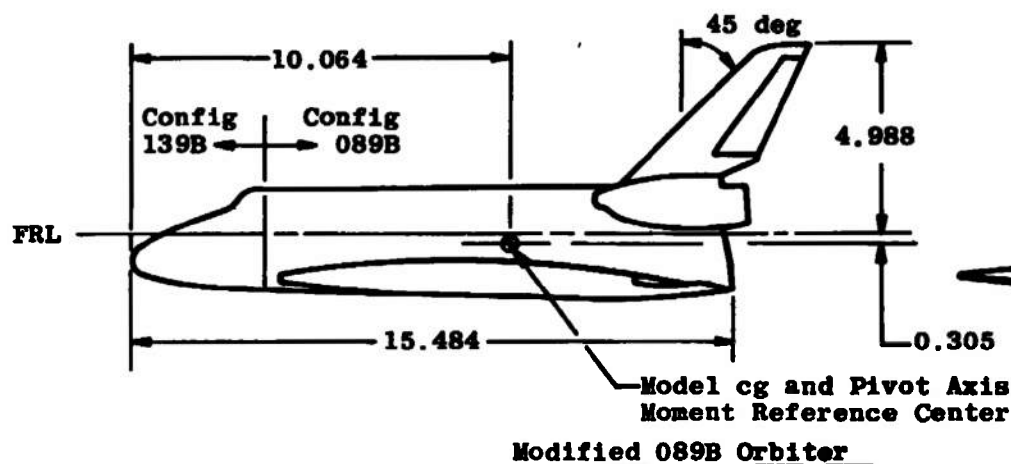
Figure 1. Model photograph.

Reference Dimensions

	0.012-Model Scale	Full Scale
Wing Area	0.38736 ft^2	2690 ft^2
Span	11.2402 in.	936.68 in.
M.A.C.	5.6976 in.	474.8 in.
Length	15.4836 in.	1290.3 in.

Configuration Nomenclature

1 - Orbiter

2 - Orbiter without Vertical Tail

11.240

40 deg

FRL - Flight Reference Line

10.064

Config 139B

Config 089B

FRL

15.484

Model cg and Pivot Axis Moment Reference Center

45 deg

4.988

0.305

Modified 089B Orbiter

All Dimensions in Inches

Figure 2. Model details.
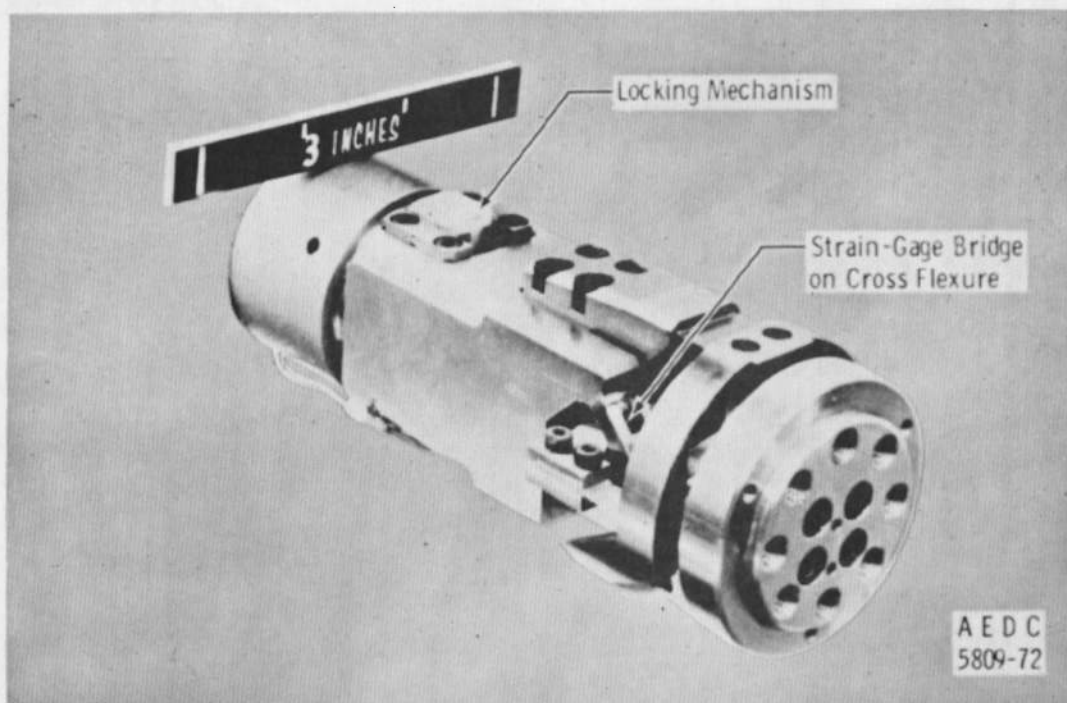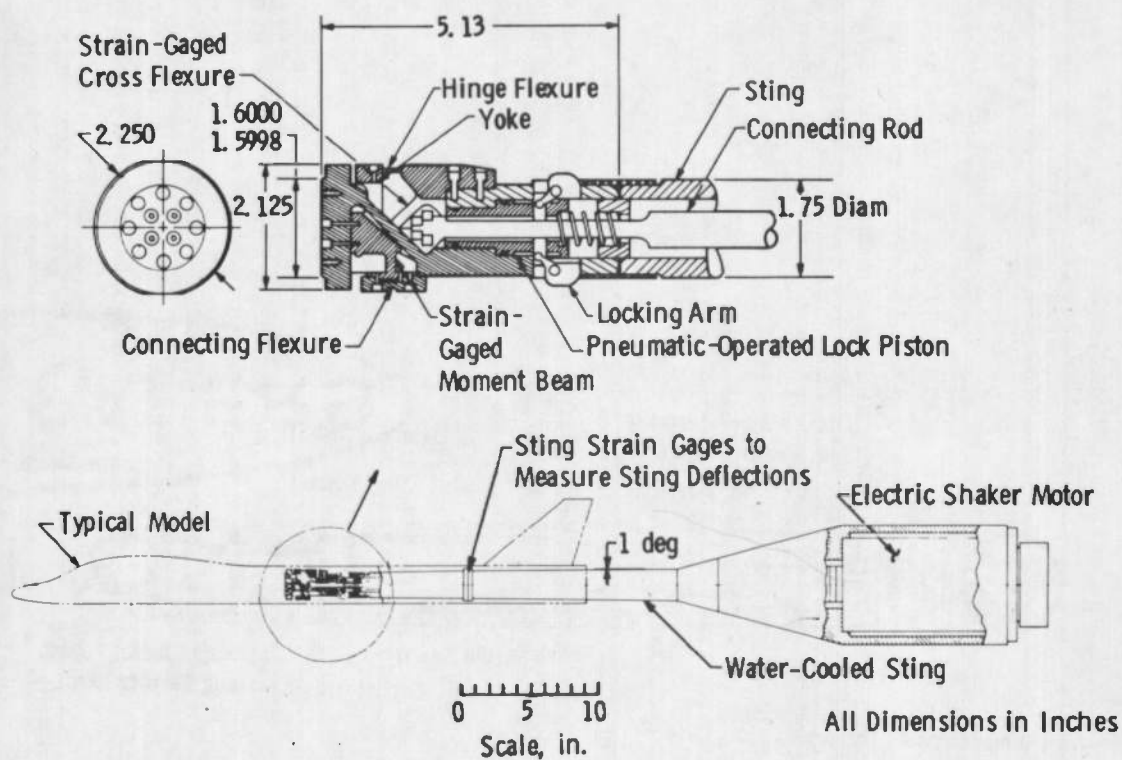
Figure 3. Pitch-/yaw-damping test mechanism (VKF 1.B).

Ali Dimensions in Inches
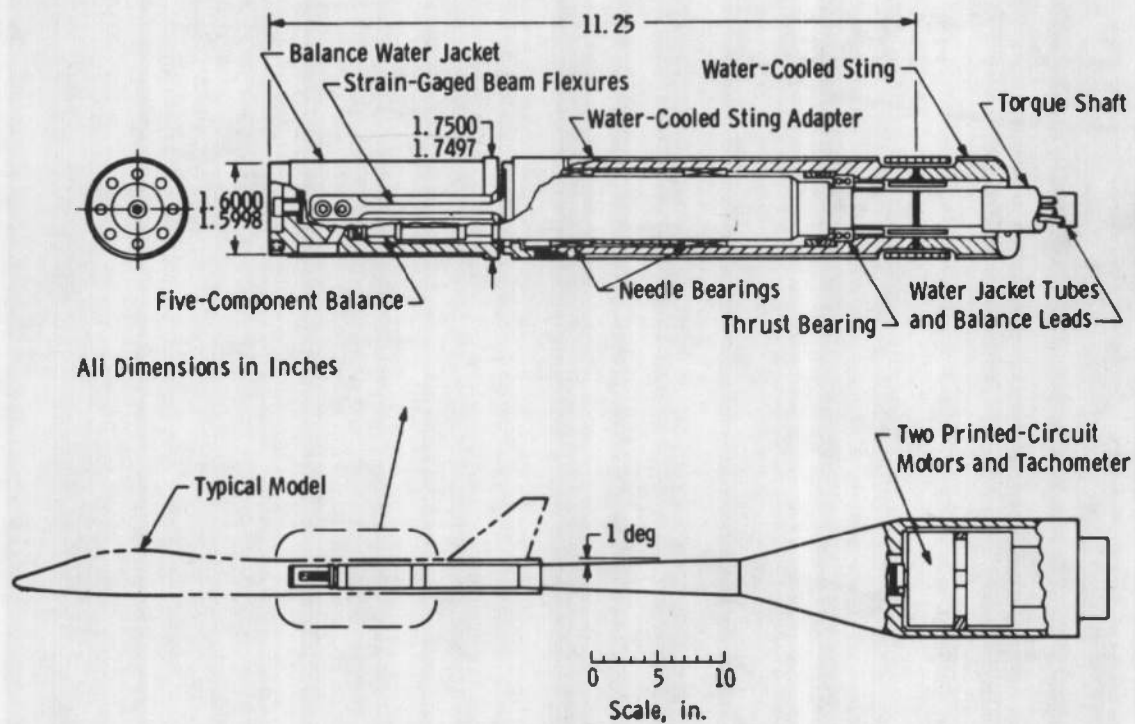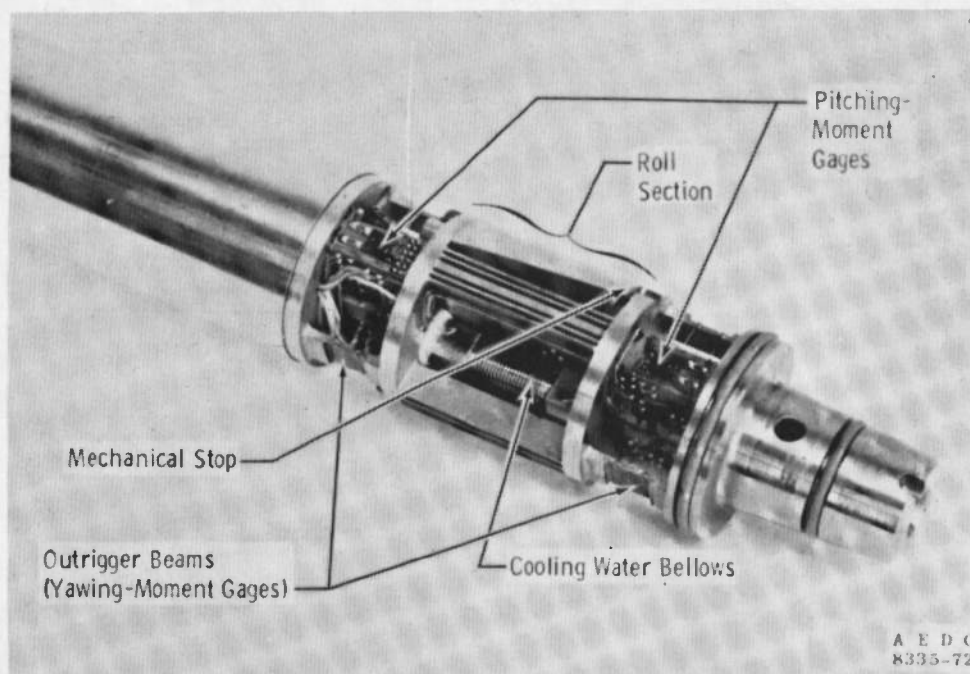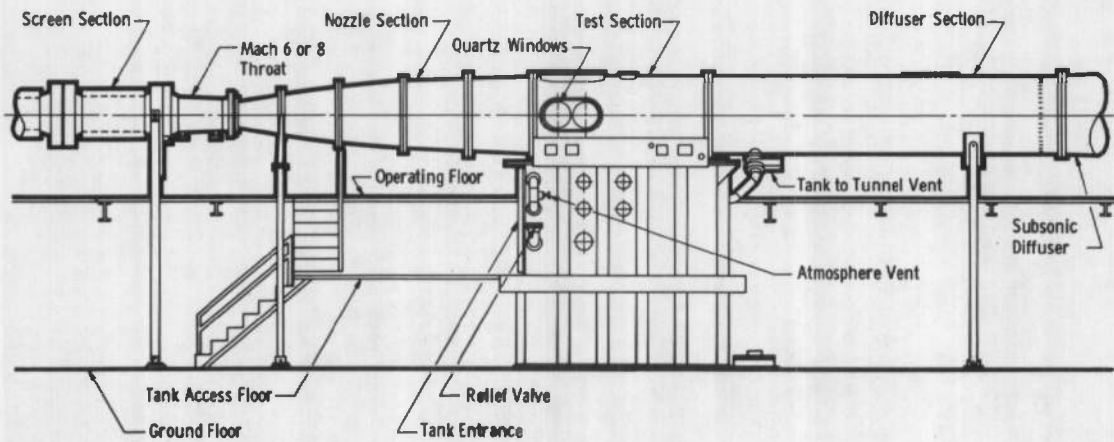
a. Test mechanism
Figure 4. Roll-damping test mechanism (VKF 1.D).

18
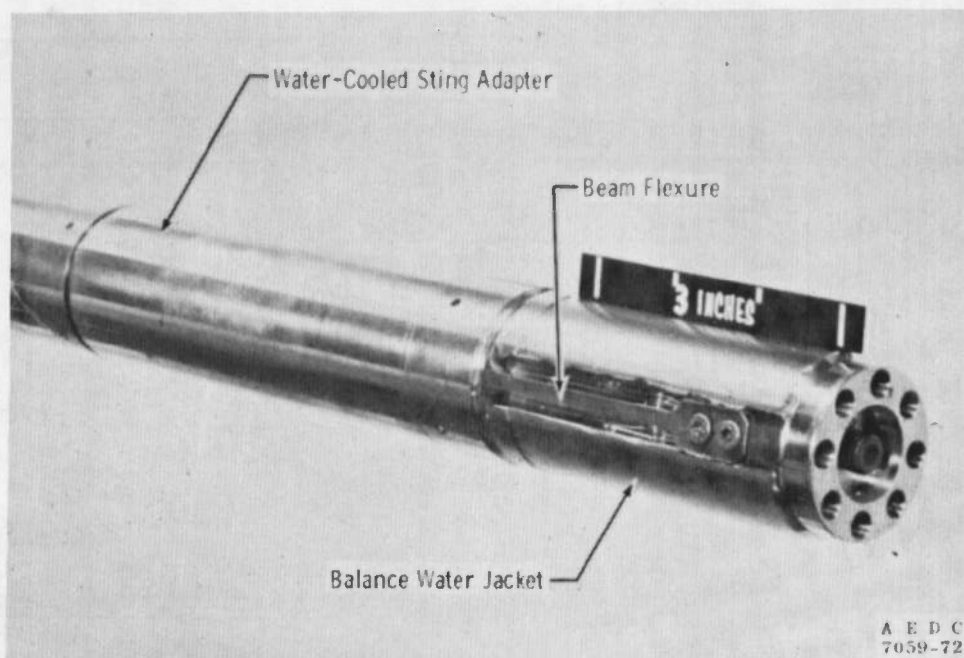
b. Photograph of the flexures and water jacket

c. Photograph of the balance
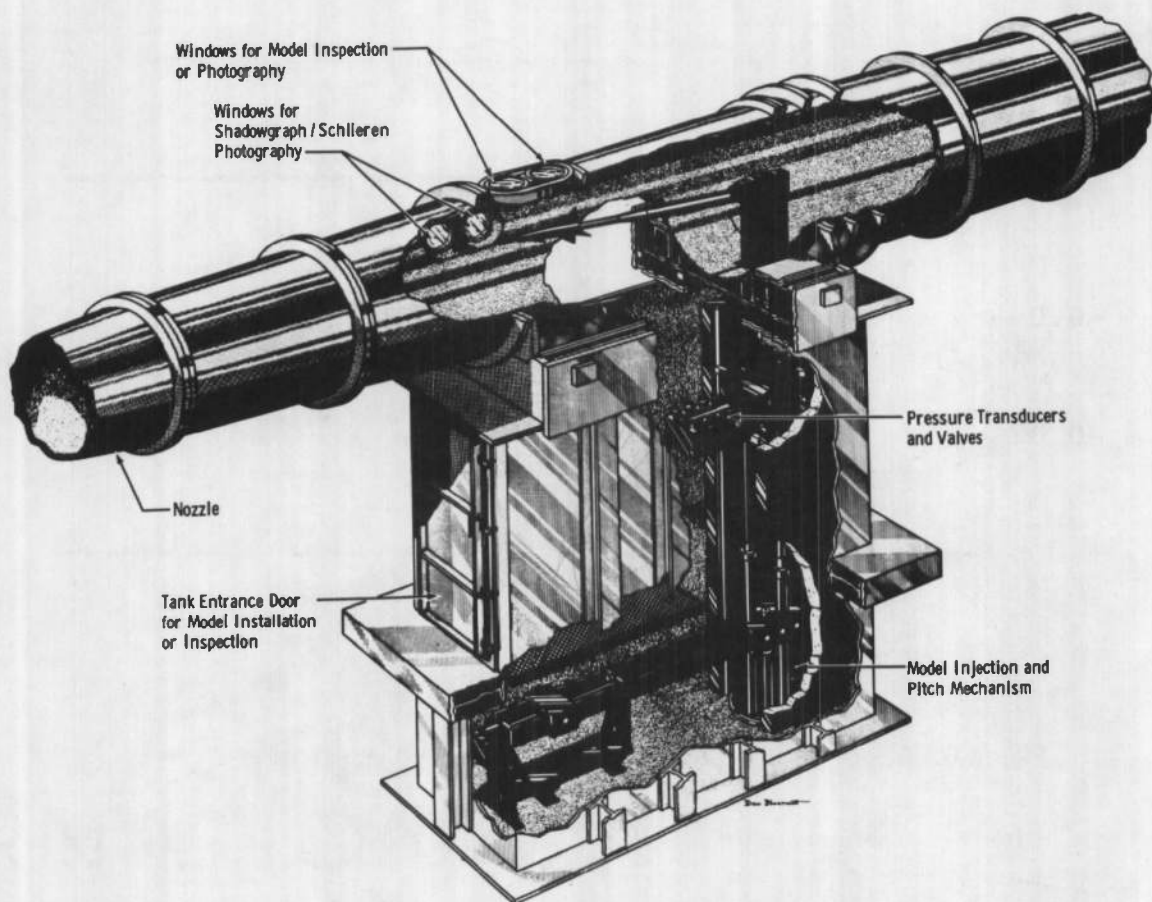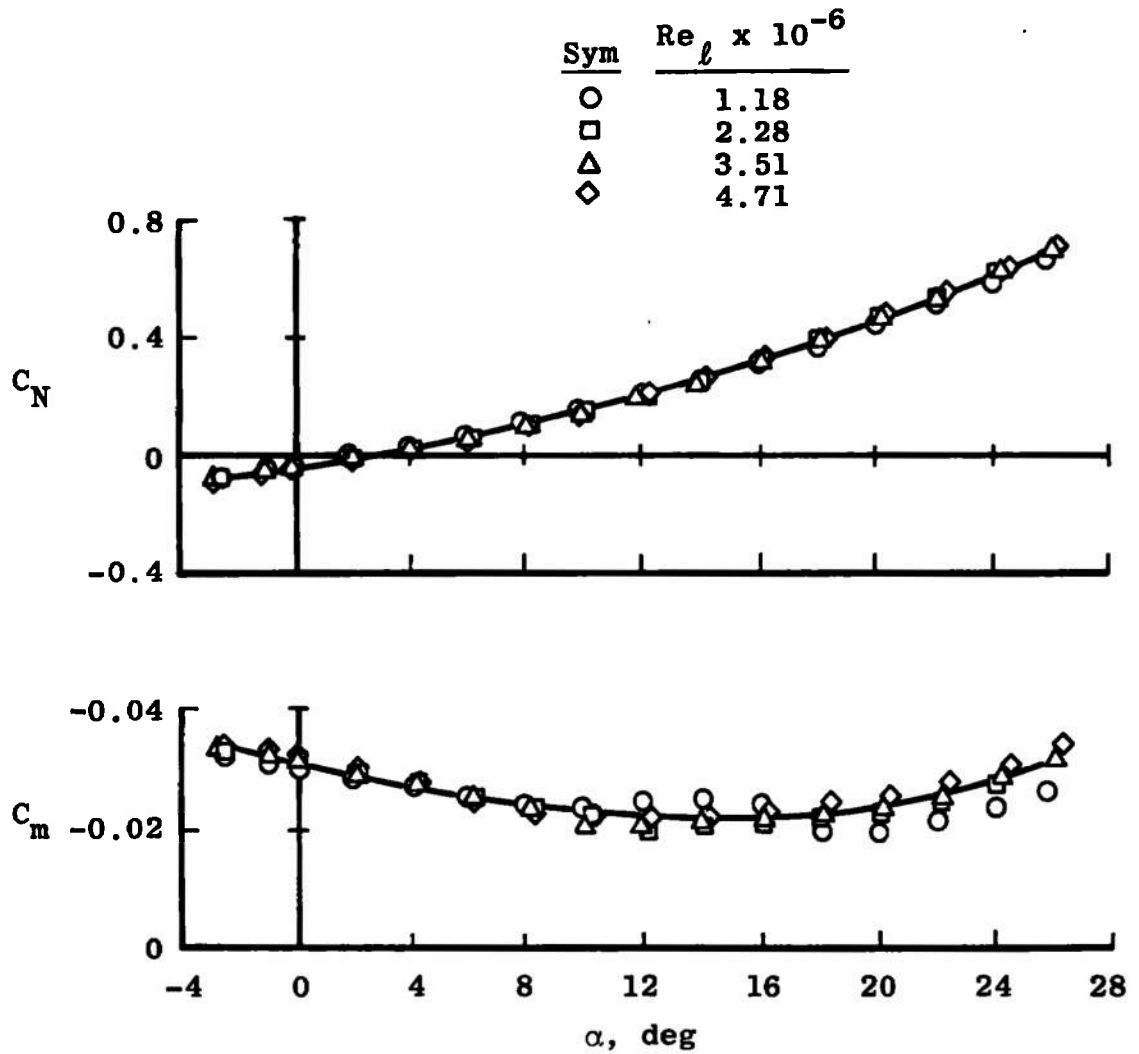Figure 4. Concluded.

Screen Section
Mach 6 or 8 Throat
Nozzle Section
Quartz Windows
Test Section
Diffuser Section
Operating Floor
Tank to Tunnel Vent
Atmosphere Vent
Subsonic Diffuser
Tank Access Floor
Ground Floor
Relief Valve
Tank Entrance

a. Tunnel assembly

Windows for Model Inspection or Photography
Windows for Shadowgraph / Schlieren Photography
Nozzle
Tank Entrance Door for Model Installation or Inspection
Pressure Transducers and Valves
Model Injection and Pitch Mechanism

b. Tunnel test section
Figure 5. Tunnel B details.

20

Sym	$Re_\ell \times 10^{-6}$
○	1.18
□	2.28
△	3.51
◇	4.71

a. Configuration 1

Figure 6. Effect of Reynolds number on the static coefficients, $M_\infty = 8$.

21
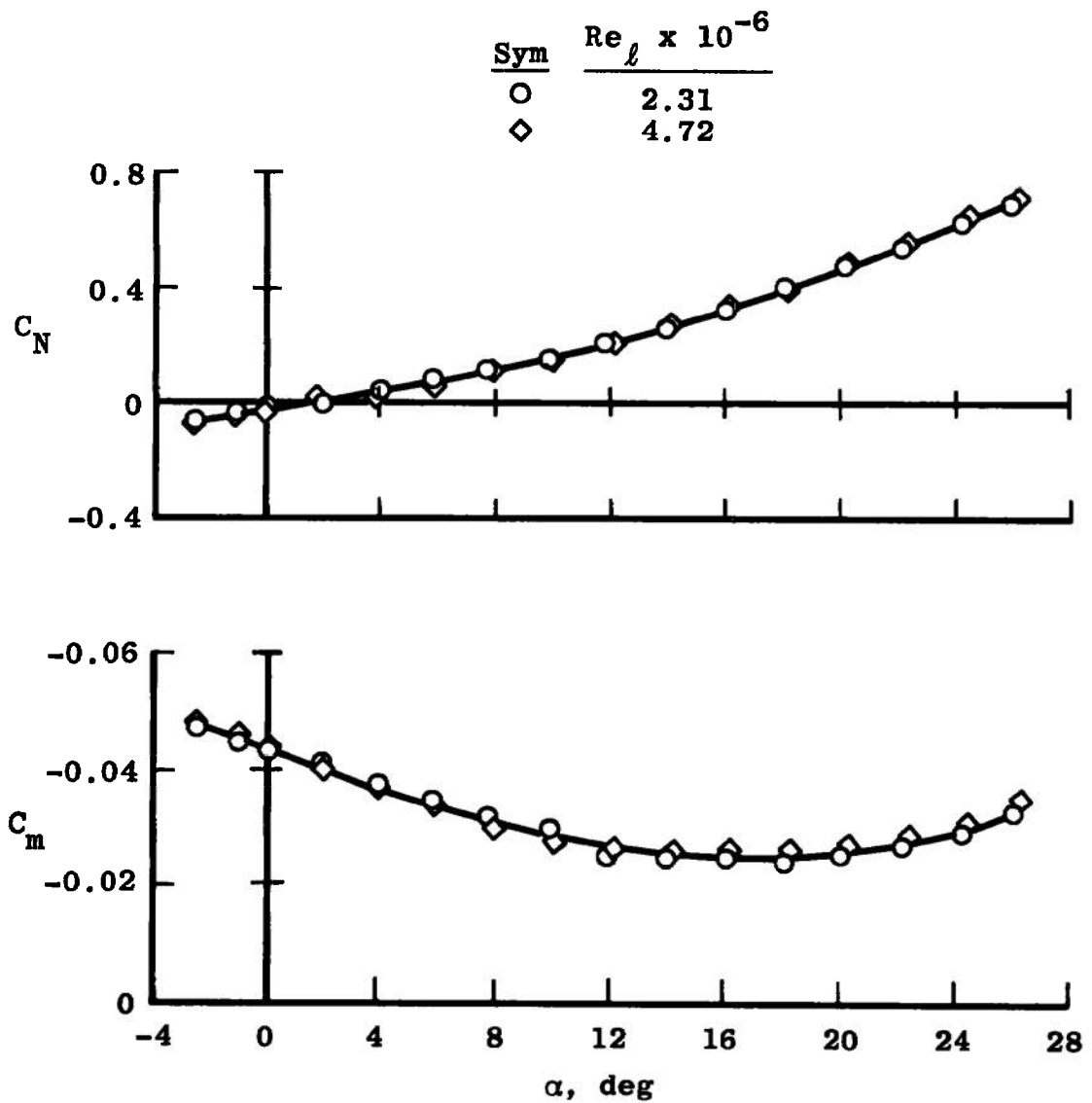
b. Configuration 2 (without vertical tail)
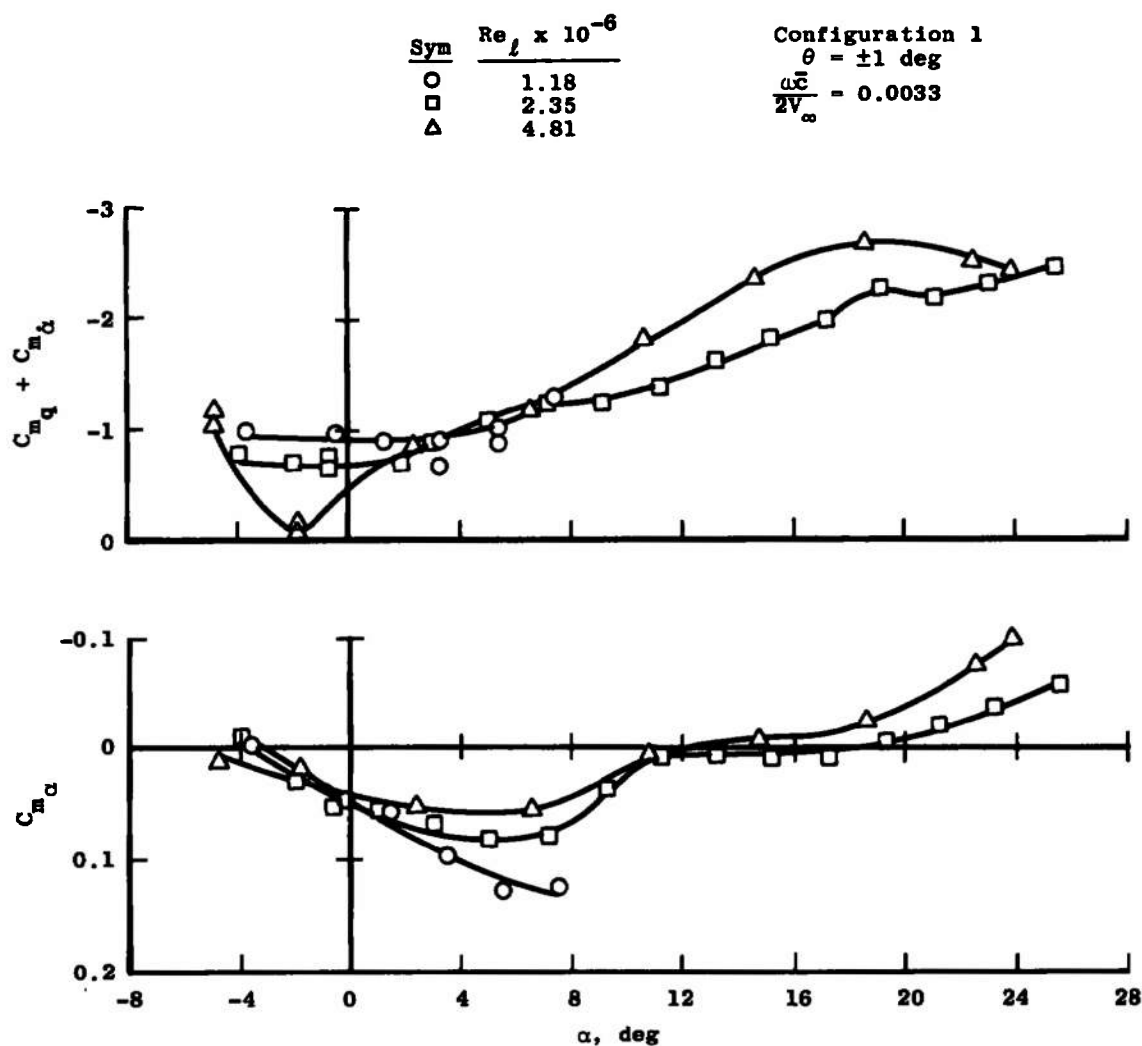Figure 6. Concluded.

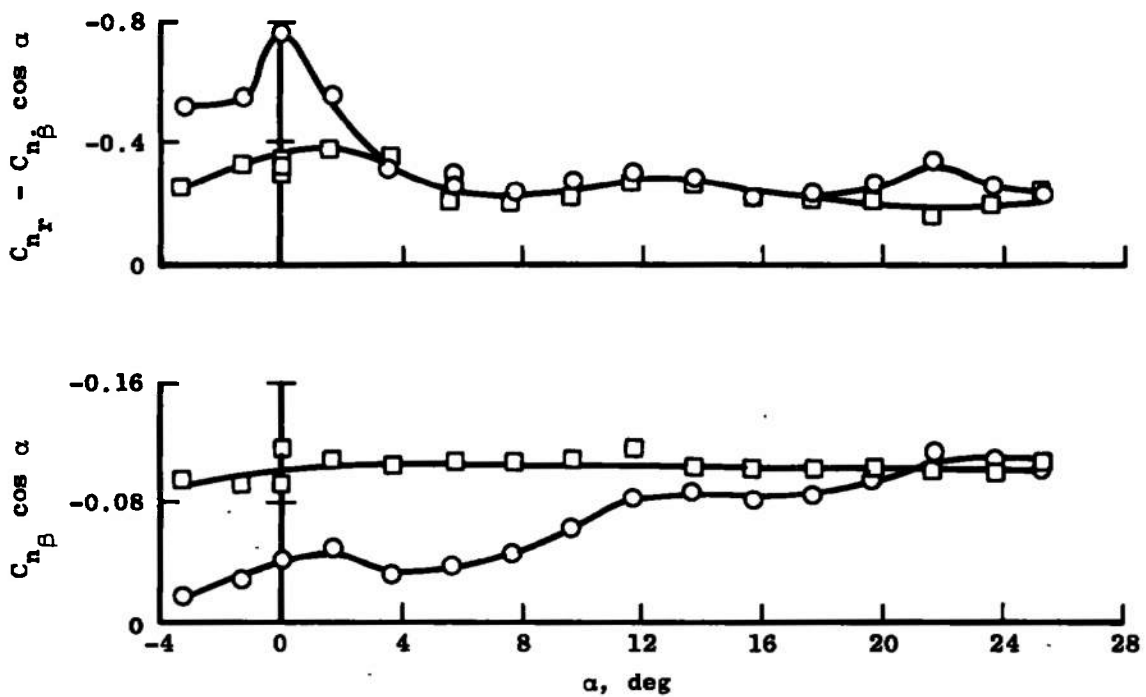Figure 7. Pitch-stability derivatives as a function of angle of attack, $M_\infty = 8$.

23

Figure 8. Yaw-stability derivatives as a function of angle of attack, $M_\infty = 8$.
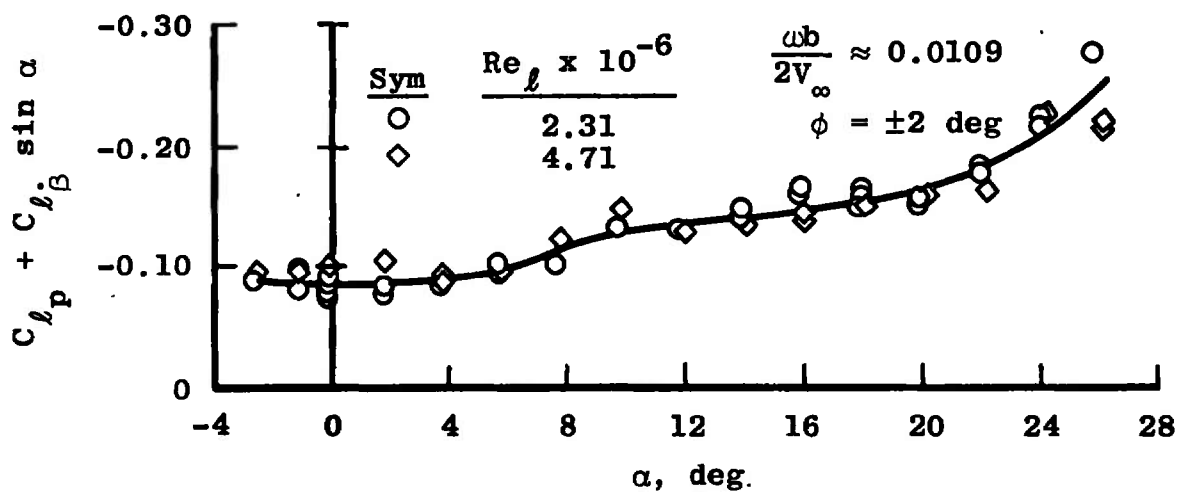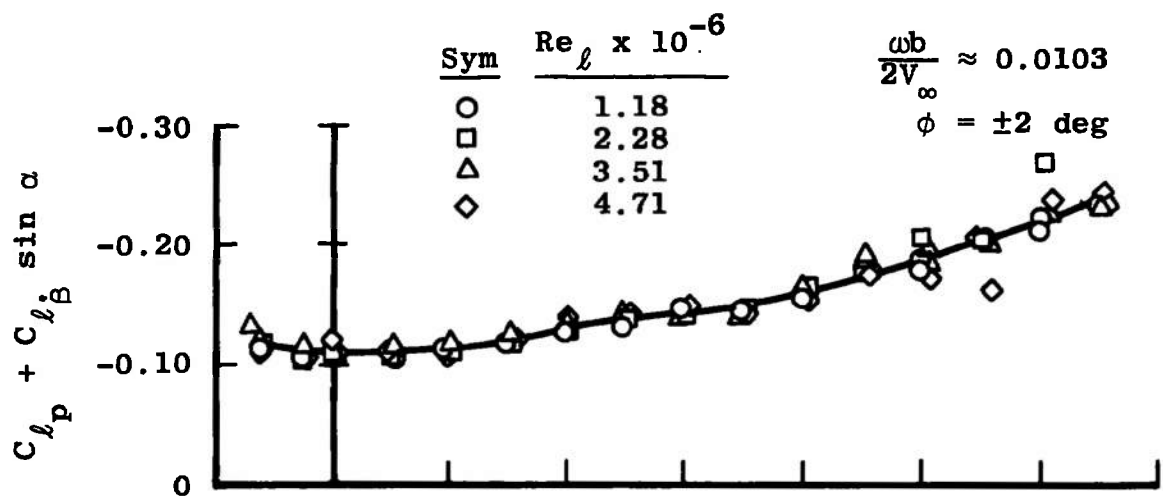
a. Configuration 1

b. Configuration 2 (without vertical tail)

Figure 9. Roll-damping derivatives as a function of angle of attack, $M_\infty = 8$.

Sym	Configuration	$\pm\phi$, deg
O	1	2
□	2 (without Vertical Tail)	2
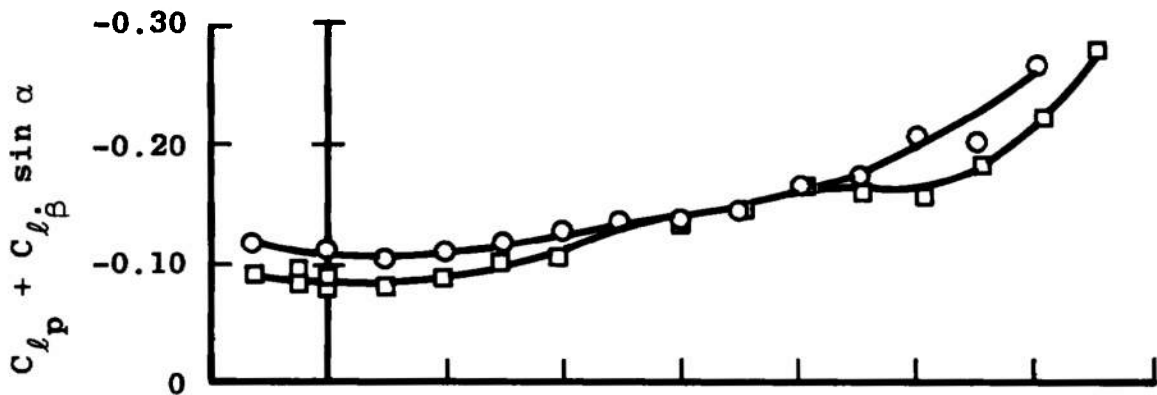
a. $Re_\ell = 2.3 \times 10^6$

b. $Re_\ell = 4.7 \times 10^6$

Figure 10. Effect of vertical tail on the roll-damping derivatives, $M_\infty = 8$.

26

Sym	Test Facility	$Re_\ell \times 10^{-6}$	α, deg
⊙	NASA–Langley (Ref. 2)	4.4	≈0
O	AEDC	4.7*	≈0

*Except Where Noted

Sym	$\omega \bar{c}/2V_\infty$	θ, deg
⊙	≈0.003 to 0.004	±1
O	≈0.003	±1

Sym	$\omega b/2V_\infty$	ψ, deg
⊙	≈0.008 to 0.012	±1
O	≈0.006	±1

$(Re_\ell = 2.3 \times 10^6)$

Sym	$\omega b/2V_\infty$	ϕ, deg
⊙	≈0.015 to 0.022	±2.3
O	≈0.010	±2.0
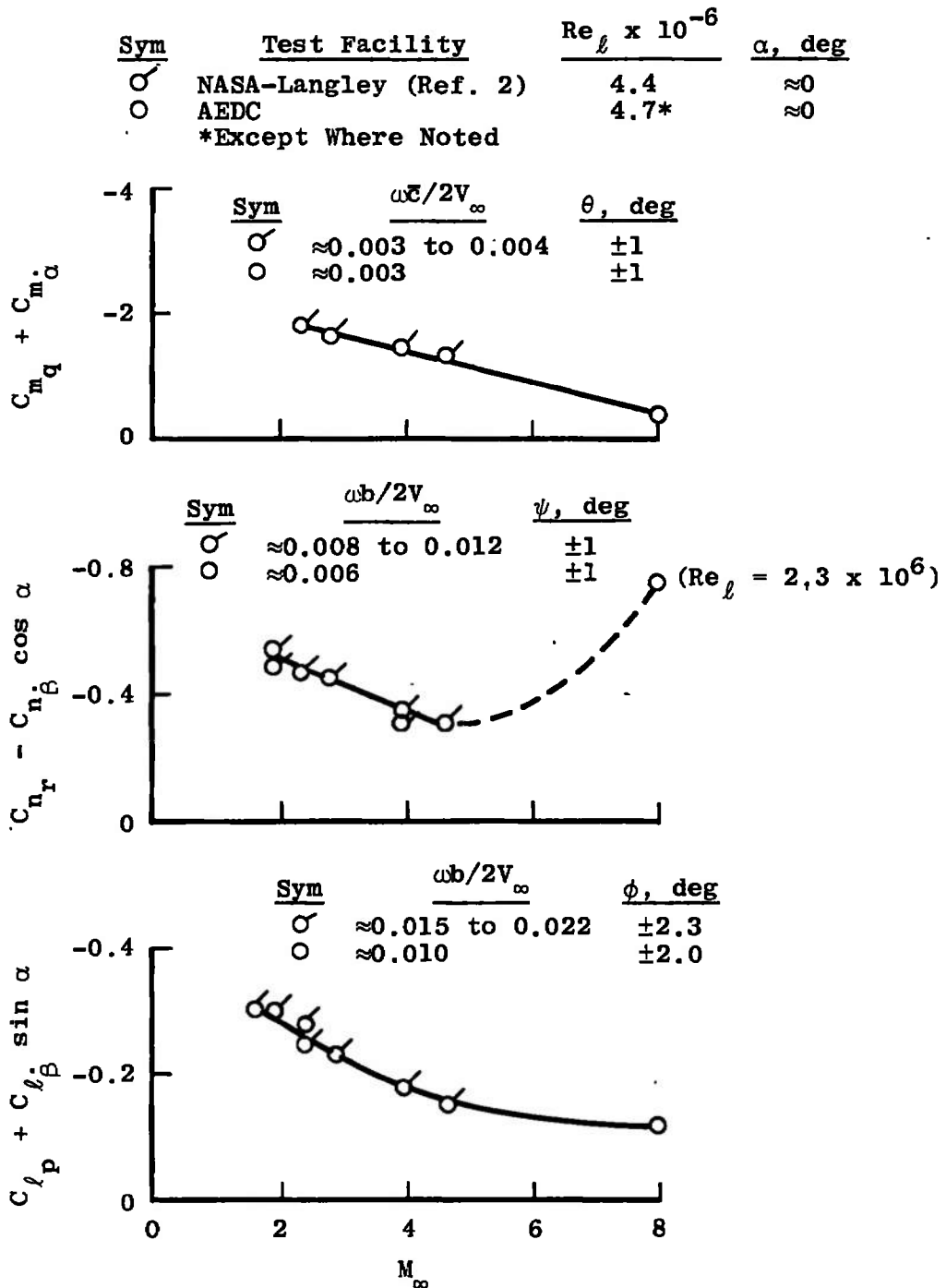
a. Configuration 1

Figure 11. Damping derivatives as a function of Mach number.
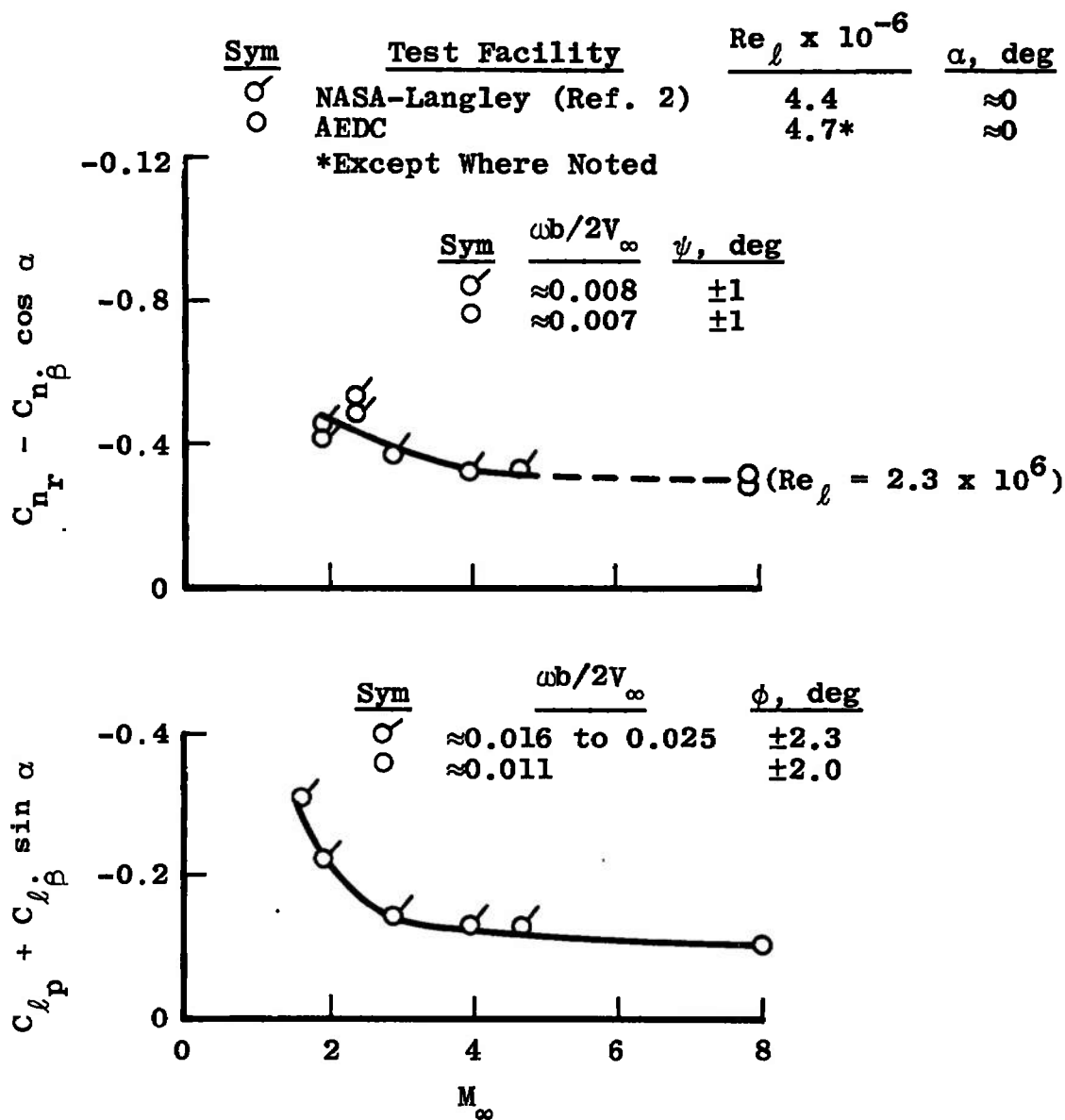
b. Configuration 2 (without vertical tail)
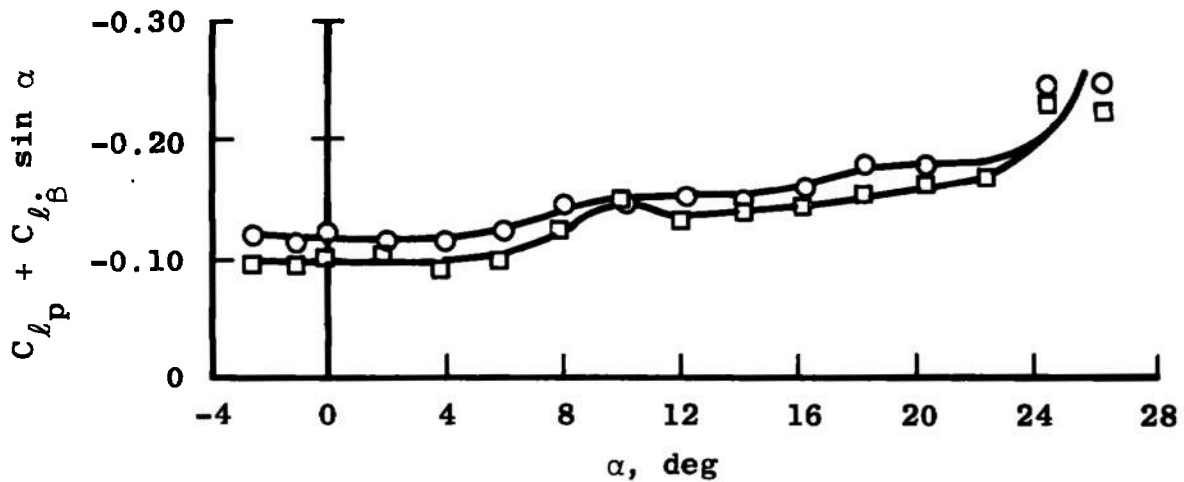Figure 11. Concluded.

a. Configuration 1

Figure 12. Yawing-moment derivatives due to roll rate as a function of angle of attack, $M_\infty = 8$.
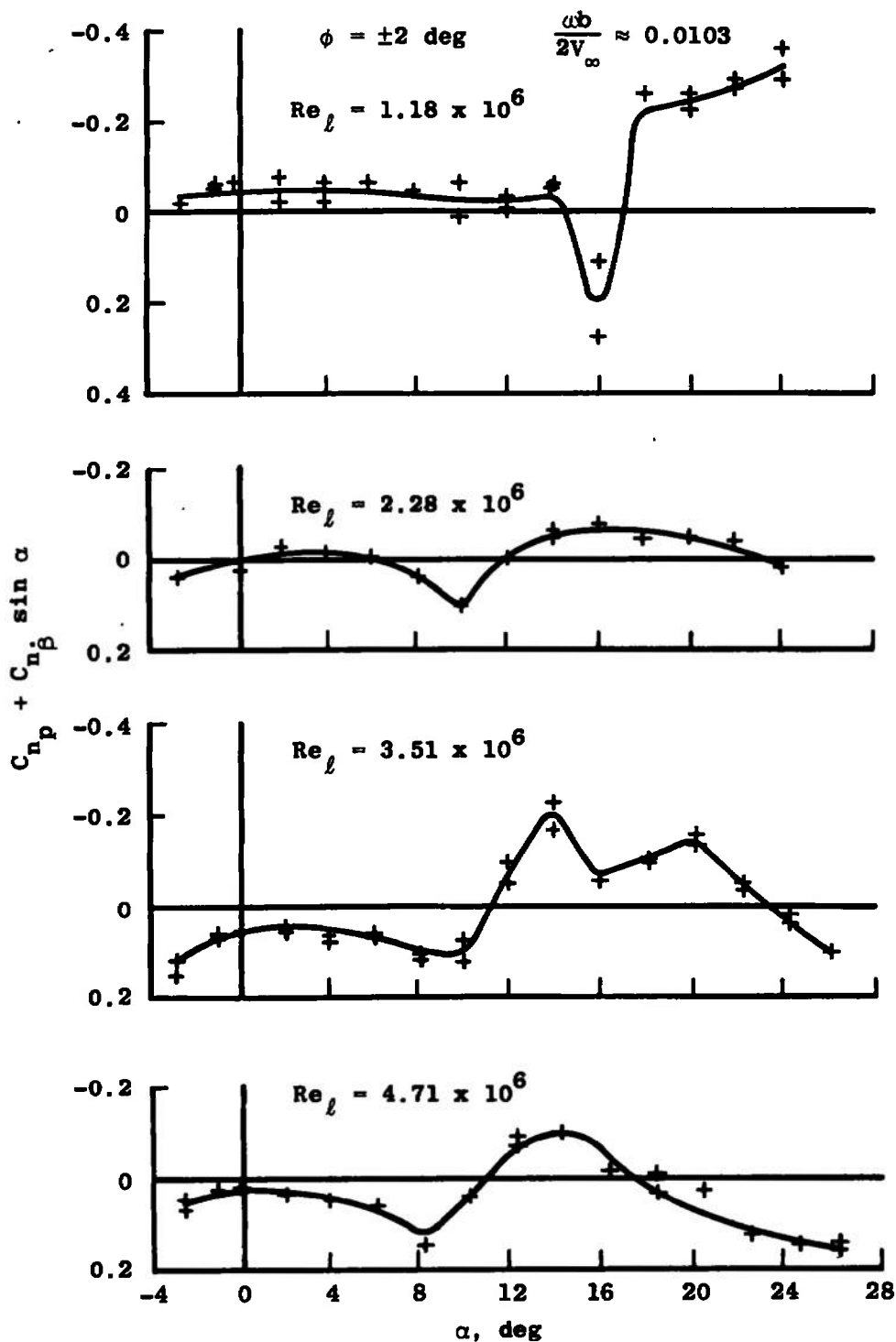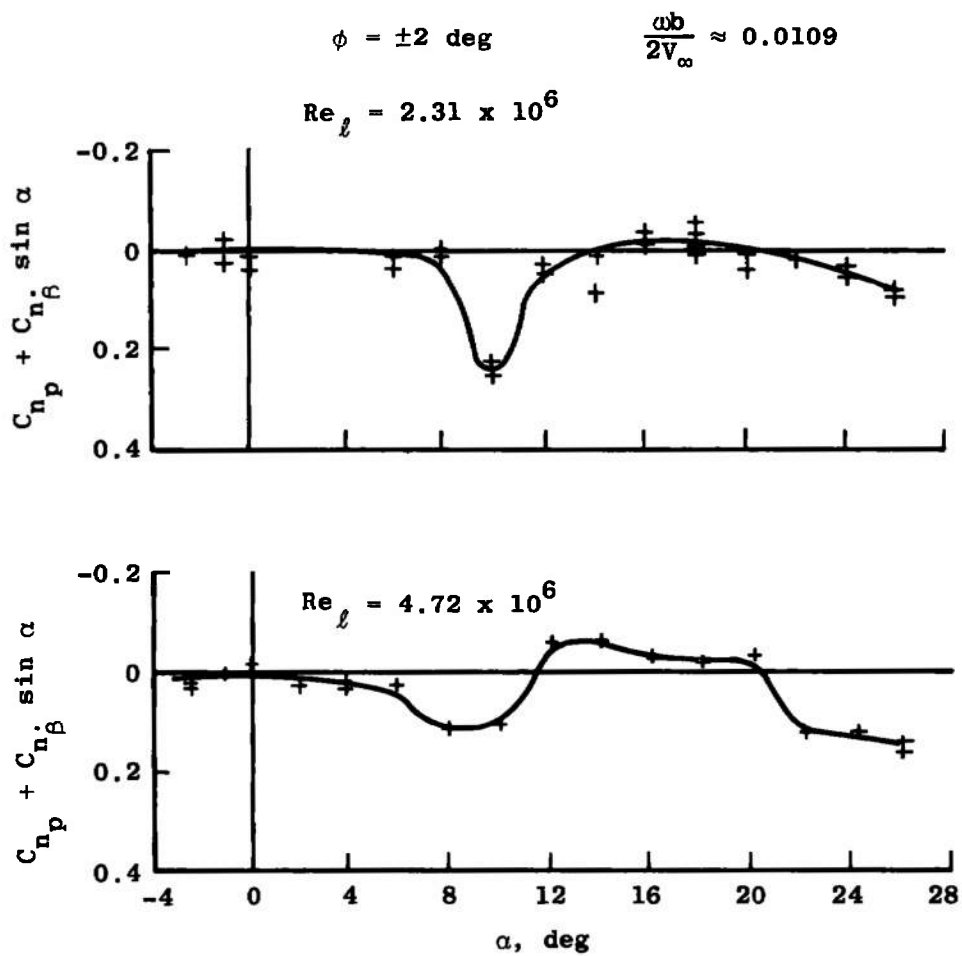
b. Configuration 2 (without vertical tail)
Figure 12. Concluded.

Table 1. Tunnel Conditions for Pitch-, Yaw-, and Roll-Damping Tests

Test Condition	M_∞	$Re_\ell \times 10^{-6}$	$p_O,$ psia	$T_O,$ °R	$q_\infty,$ psia	$V_\infty,$ ft/sec
A	7.95	1.18	200	1310	0.945	3819
B	7.98	2.35	401	1314	1.862	3826
C	7.99	3.52	600	1308	2.767	3818
D	8.00	4.73	851	1358	3.906	3890
E	8.00	4.82	849	1335	3.894	3857

Table 2. Test Summaries

Pitch-Damping Tests

Configuration	Test Condition*	$\omega\bar{c}/2V_\infty \times 10^3$	α range, deg
1	D	3.40	24
1	A	3.34	-3.7 to 7.4
1	B	3.34	-4.1 to 25.9
1	E	3.32	-4.9 to 23.9

Yaw-Damping Tests

Configuration	Test Condition*	$\omega b/2V_\infty \times 10^3$	α range, deg
1	B	6.27	-3.3 to 25.3
2	B	6.60	-3.4 to 25.3

Roll-Damping Tests

Configuration	Test Condition*	$\omega b/2V_\infty \times 10^3$	α range, deg
1	D	10.2	-3.1 to 26.5
1	C	10.4	-2.9 to 26.1
1	B	10.4	-2.5 to 26.0
1	A	10.4	-2.5 to 25.8
2	B	11.0	-2.6 to 26.0
2	D	10.8	-2.6 to 26.2

*As defined in Table 1.

31

NOMENCLATURE

A	Reference area, model wing area, 0.38736 ft^2
b	Reference length for lateral coefficients, wing span, 0.93668 ft
C_ℓ	Rolling-moment coefficient, rolling moment/$q_\infty Ab$
C_{ℓ_p}	Rolling-moment coefficient due to roll velocity $\partial(C_\ell)/\partial(pb/2V_\infty)$, radian^{-1}
$C_{\ell_{\dot{\beta}}}$	Rolling-moment coefficient due to rate of change of sideslip angle, $\partial(C_\ell)/\partial(\dot{\beta}b/2V_\infty)$, radian^{-1}
C_m	Pitching-moment coefficient, pitching moment/$q_\infty A\bar{c}$
C_{m_q}	Pitching-moment coefficient due to pitch velocity, $\partial(C_m)/\partial(q\bar{c}/2V_\infty)$, radian^{-1}
C_{m_α}	Pitching-moment coefficient due to angle of attack, $\partial(C_m)/\partial\alpha$, radian^{-1}
$C_{m_{\dot{\alpha}}}$	Pitching-moment coefficient due to rate of change of angle of attack, $\partial(C_m)/\partial(\dot{\alpha}\bar{c}/2V_\infty)$, radian^{-1}
C_N	Normal-force coefficient, normal force/$q_\infty A$
C_n	Yawing-moment coefficient, yawing moment/$q_\infty Ab$
C_{n_p}	Yawing-moment coefficient due to roll rate, $\partial(C_n)/\partial(pb/2V_\infty)$, radian^{-1}
C_{n_r}	Yawing-moment coefficient due to yaw velocity, $\partial(C_n)/\partial(rb/2V_\infty)$, radian^{-1}
C_{n_β}	Yawing-moment coefficient due to sideslip angle, $\partial(C_n)/\partial\beta$, radian^{-1}
$C_{n_{\dot{\beta}}}$	Yawing-moment coefficient due to rate of change of sideslip angle, $\partial(C_n)/\partial(\dot{\beta}b/2V_\infty)$, radian^{-1}
C_Y	Side-force coefficient, side force/$q_\infty A$
C_{Y_p}	Side-force coefficient due to roll velocity, $\partial(C_Y)/\partial(pb/2V_\infty)$, radian^{-1}
$C_{Y_{\dot{\beta}}}$	Side-force coefficient due to rate of change of sideslip angle, $\partial(C_Y)/\partial(\dot{\beta}b/2V_\infty)$, radian^{-1}

$\bar{c}$	Reference length for longitudinal coefficients, wing mean aerodynamic chord, 0.4748 ft
ℓ	Model length (reference length for Reynolds number), 1.2903 ft
M_∞	Free-stream Mach number
p	Rolling velocity, radians/sec
p_O	Tunnel stilling chamber pressure, psia
q	Pitching velocity, radians/sec
q_∞	Tunnel free-stream dynamic pressure, psfa or psia
Re_ℓ	Tunnel free-stream Reynolds number based on model length (ℓ)
r	Yawing velocity, radians/sec
T_O	Tunnel stilling chamber temperature, °R
V_∞	Tunnel free-stream velocity, ft/sec
α	Angle of attack, deg or radian
β	Sideslip angle, radian
$\Delta(\ )$	Uncertainty band (95-percent confidence limit)
θ	Angular displacement in pitch, deg
ϕ	Angular displacement in roll, deg
ψ	Angular displacement in yaw, deg
ω	Model angular oscillation frequency, radians/sec
$\dfrac{\omega b}{2V_\infty}$	Reduced frequency parameter for the yaw-and roll-damping tests, radian
$\dfrac{\omega \bar{c}}{2V_\infty}$	Reduced frequency parameter for the pitch-damping tests, radian
$(\dot{\ })$	First derivative with respect to time